A THESIS FOR THE DEGREE OF
MASTER OF SCIENCE IN FOOD AND NUTRITION

Intestinal microbiome profiling in *Ido1*$^{-/-}$ mice of colitis model

대장염 모델 *Ido1*$^{-/-}$ 마우스에서의 장내 미생물체 분석

August, 2014

Department of Food and Nutrition
Graduate School
Seoul National University
Ji Hee Shin

Intestinal microbiome profiling in *Ido1*$^{-/-}$ mice of colitis model

대장염 모델 *Ido1*$^{-/-}$ 마우스에서의 장내 미생물체 분석

지도교수 신 동 미

이 논문을 생활과학석사 학위논문으로 제출함

2014 년 4 월

서울대학교 대학원
식품영양학과
신 지 희

신지희의 생활과학 석사학위 논문을 인준함

2014 년 6 월

위 원 장 _____ (인)

부위원장 _____ (인)

위 원 _____ (인)

Abstract

Intestinal microbiome profiling in *Ido1*$^{-/-}$ mice of colitis model

Ji Hee Shin
Department of Food and Nutrition
The Graduate School
Seoul National University

Intestinal commensal bacteria get growing attention due to their beneficial roles in the host immune system. We proposed to test the hypothesis that tryptophan metabolism mediates the interaction between intestinal commensal bacteria and host inflammatory responses, using *Ido1* (indoleamine 2,3-dioxygenase 1; a rate-limiting enzyme in tryptophan metabolism) knock-out (*Ido1*$^{-/-}$) mice and wild-type (*Ido1*$^{+/+}$) mice. Mouse inflammatory bowel disease (IBD) model was induced by dextran sodium sulfate (DSS) treatment. Both *Ido1*$^{-/-}$ and *Ido1*$^{+/+}$ mice developed colitis by 2% DSS treatment; however, *Ido1*$^{+/+}$ mice developed much more severe colonic inflammation compared with *Ido1*$^{-/-}$ mice. Especially, colon lengths were shortened and histological scores were higher in *Ido1*$^{+/+}$ mice than *Ido1*$^{-/-}$ mice. Metagenomic analysis was performed to identify any changes in colonic microbiome profiles between two different genotypes. 16S ribosomal RNA (16S rRNA) pyrosequencing analysis revealed that distinct distribution of eight phyla were observed between *Ido1*$^{-/-}$ and *Ido1*$^{+/+}$ mice. Interestingly, ratio of Bacteroidetes to Firmicutes was

significantly different in those two groups of mice. *Ido1*$^{-/-}$ mice turned out to have more *Bacteroides, Parabacteroides, Barnesiella, Prevotella.* Three out of these four bacteria are known to use tryptophan to produce indole. In *Ido1*$^{+/+}$ mice, *Mucispirillum,* which utilize mucin and *Escherichia/Shigella,* which well known as pathogenic bacteria, was particularly high. Overall, these results suggest that *Ido1* plays roles in development of mouse inflammatory bowel disease (IBD) through alteration of intestinal commensal bacteria profiles. Our findings provide one of the evidences that host system intestinal microbiota may communicate by sharing nutrient metabolism networks.

Key words: Gut microbiome, Indoleamine 2,3-dioxygenase1 (*Ido1*), Tryptophan, Pyrosequencing, Dextran sodium sulfate (DSS), Colitis

Student Number: 2012-21496

Contents

List of Tables

List of Figures

List of Abbreviations

DAI	disease activity index
DSS	dextran sodium sulfate
IBD	inflammatory bowel disease
IDO	indoleamine 2,3-dioxygenase
KO	knock-out
OTU	operational taxonomic unit
SPF	specific pathogen free
TNBS	trinitrobenzene sulfonic acid
WT	wild-type
16S rRNA	16S ribosomal RNA

I . Introduction

The human body has a large number of microorganisms—such as a bacteria, fungi, viruses—that live in and on our bodies. Bacterial genomes are estimated to outnumber human genomes by a factor of 100 in the distal gut (Backhed, Ley, Sonnenburg, Peterson, & Gordon, 2005; Gill et al., 2006). These have been referred to as "the forgotten organ," due to their biological function and complexity being similar to an organ (O'Hara & Shanahan, 2006).

Recently, researchers have been able to study a variety of gut microbial communities through culture-independent molecular methods, such as denaturing gradient gel electrophoresis (DGGE), terminal restriction fragment length polymorphism (T-RFLP), quantitative PCR, and pyrosequencing. These methods are based on analysis of bacterial 16S ribosomal RNA (16S rRNA) gene sequences (Shendure & Ji, 2008). Pyrosequencing, also known as next-generation sequencing (NGS), is a useful technique for developing our understanding of complex microbial communities. Many researchers have studied NGS-based intestinal microbiota profiles in particular diseases.

Since gut microbiota play a decisive role in the mucosal immune system, many studies have demonstrated that intestinal disease and health are based on the presence or absence of gut flora (Archambaud et al., 2013; Maslowski et al., 2009; Neufeld, Kang, Bienenstock, & Foster, 2011). In particular, an immune system imbalance, which is caused by dysbiosis of the intestinal microbiota, is one of the pathogenesis in inflammatory bowel disease (IBD) (Sartor, 2008). It is more severe in germ-free

mice than in specific pathogen–free (SPF) mice in a mouse model of IBD. This result is caused by IL-10, anti-inflammatory cytokine, which is necessarily induced by gut microbiota (Pils et al., 2011).

Chemically-induced mouse models of IBD are one of the most commonly used models. These include trinitrobenzene sulfonic acid (TNBS), oxazolone, and dextran sodium sulfate (DSS). Among these models, dextran sodium sulfate (DSS)-induced colitis is widely used in studies for IBD. However, the mechanisms of DSS are not yet wholly known, and may increase the infiltration of harmful bacteria or tight junction disruption in mucus layers (Johansson et al., 2010). Therefore, based on these mechanisms, this study used a colitis model induced by the use of DSS that can study how intestinal microorganisms directly affect diseases.

In current years, not only have commensal bacteria been studied for their role in causing diseases, but also as a guide for diagnosis and treatment (Allegretti & Hamilton, 2014; Swidsinski, Loening-Baucke, Vaneechoutte, & Doerffel, 2008). Many factors, such as the genotype of the host, lifestyle, and the drug responsible for varying the gut flora have been examined. Among them, diet has been a critical influence on the changes in the intestinal microbiota (Kau, Ahern, Griffin, Goodman, & Gordon, 2011). According to a recent study, changes in the gut microbiota caused by a high-fat diet could reduce the expression levels of the gene that is involved in tight junctions, resulting in an increase in intestinal bacteria permeability (Cani et al., 2008). Regarding the issue of diet and intestinal bacteria, studies using animal models with deficiency of a particular nutrient metabolism are needed to be done.

A recent interesting article presented that changes of intestinal microorganisms are dependent on whether certain enzymes are deficient in the host of the disease.

Hashimoto et al. showed that a lack of the angiotensin-I-converting enzyme 2 (*Ace2*) gene in DSS-induced colitis mice resulted in a significantly higher seriousness of the disease than the normal mice, but when the mice were fed a tryptophan-supplement diet, the disease was alleviated to a remarkable degree. In addition, by showing that the recurrence of colitis happened in mice that had received transplants of gut microorganisms for *Ace2*-deficient mice, the study explained that a change in the gut microorganisms associated with the genotype of the host has a direct impact on the disease (Hashimoto et al., 2012). It is an impressive study on the relationship between the immune responses, which are mediated by commensal bacteria, diet, and the genotype of the host. In particular, amino acids have been known to maintain the health of the gut (Wang, Qiao, & Li, 2009). Several studies have looked into the complexity of the commensal bacteria, but we are still missing a clear result for the relationship between intestinal microorganisms and tryptophan metabolism.

Tryptophan, which is an essential amino acid, has a therapeutic effect by decreasing the expression level of pro-inflammatory cytokine against DSS-induced colitis (Kim et al., 2010; Shizuma, Mori, & Fukuyama, 2013). Based on the two research projects, it can be seen that there is a close relationship between gut immunity and tryptophan mediated by commensal bacteria; therefore, we focused on the genes that encode tryptophan-metabolizing enzymes. Tryptophan is first metabolized by a rate-limiting enzyme called Indoleamine-2,3-dioxygenase1 (*IDO1*). *IDO1* may not only play a role in the metabolism of tryptophan, but may also play pathophysiological roles in various human body functions, one of which is involved in the regulation of immune responses. For example, it has been reported that the metabolites of tryptophan, which are metabolized through the *IDO1* acts as a ligand

of the aryl hydrocarbon receptor (AhR) to mediate an immune suppressive response in DCs (Knights, Lassen, & Xavier, 2013; Nguyen et al., 2010). However, the precise role of *IDO1* in different diseases is not clearly beneficial or harmful to the host (Huttunen et al., 2010). A recent study by Troy and Kasper provided support for one theory, which proposed that mortality from endotoxic shock is decreased in *Ido1*-deficient mice (Troy & Kasper, 2010).

Itoh et al. illustrated that mice had different susceptibilities to entero-pathogenic *Escherichia coli* despite only varying the breeding environment of mouse, SPF, or conventional conditions (Itoh, Maejima, Ueda, & Fujiwara, 1979). If so, it begins to bring questions about genetic changes in mice such as how their degree of exposure to microorganisms varies depending on their breeding environment. Therefore, to address the question of whether commensal microbiota can affect host genome expressions, transcriptome analyses of SPF and conventional mice were carried out.

In our preliminary studies, despite only varying the housing environments of the mice (conventional and SPF), the gene expression profiles of the small intestines and colon were differed significantly, based on their environment. Surprisingly, amino acid metabolism was identified as a significantly modulated function, when we classified the differentially-expressed genes between conventional and SPF. It was notable that the expression of *Ido1* was increased 4.3-fold in conventional mice than SPF mice (**Figure 1. A–C**).

Along these lines, we proposed to test the hypothesis that tryptophan metabolism mediates the interaction between intestinal commensal bacteria and the host's inflammatory responses.

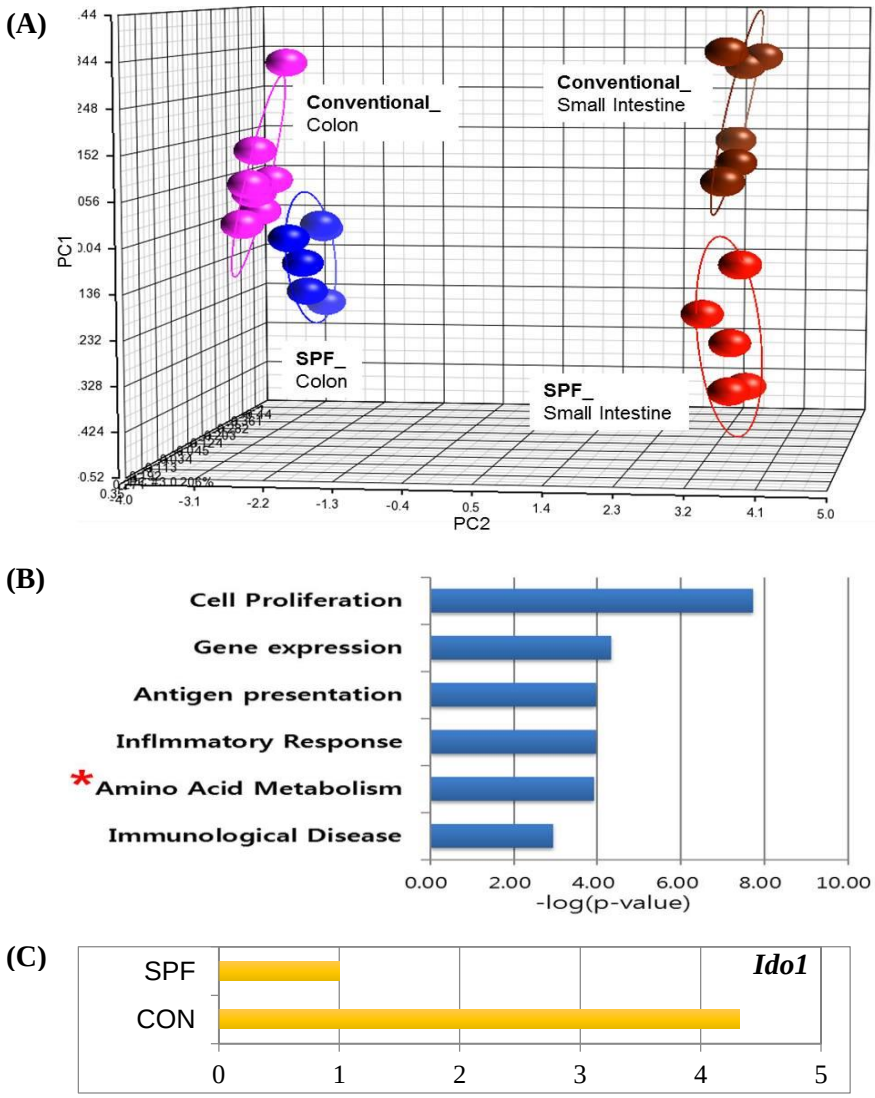

Figure 1. Transcriptome analysis of specific-pathogen-free mice and conventional mice

(A) Gene expression of the small intestine and large intestine of mice raised in conventional or SPF environment identified by principle component analysis (PCA)

(B) Classification of the biological function of statistically significant gene. *P* values were analyzed using Fisher's exact test.

(C) Difference in the *Ido1* expression level by housing environment of mouse (SPF vs. conventional).

II . Materials and Methods

1. *Animal*

C57BL/6 (*Ido1*$^{+/+}$) mice and *Ido1*$^{-/-}$ mice were purchased from Jackson Laboratory (Bar Harbor, Maine, USA). Experimental mice were 8–11 weeks old and kept in individual cages under conditions of specific pathogen free (SPF) animal facility at the Bio medical Center for Animal Resource Development (BCARD) of Seoul National University College of Medicine (Seoul, Korea).

2. *Induction of acute colitis with DSS*

Induction of acute colitis with DSS was performed according to protocol (Maxwell, Brown, Smith, Byrne, & Viney, 2009). First, C57BL/6 (*Ido1*$^{+/+}$) mice and *Ido1*$^{-/-}$ mice, which are 8-11 weeks of age, were randomly divided into six groups by DSS concentration and genotype (n=4–7 per groups). The six groups were designed as follows: (1) 0% DSS treated in *Ido1*$^{+/+}$ mice, (2) 1% DSS treated in *Ido1*$^{+/+}$ mice, (3) 2% DSS treated in *Ido1*$^{+/+}$ mice, (4) 0% DSS treated in *Ido1*$^{-/-}$ mice, (5) 1% DSS treated in *Ido1*$^{-/-}$, (6) 2% DSS treated in *Ido1*$^{-/-}$ mice. All mice were administered dextran sodium sulfate (DSS, molecular weight: 36,000-50,000Da, MP biomedicals, Santa Ana, CA, USA) dissolved in drinking water (w/v) for 7 days *ad libitum* **(Figure 2)**.

Clinical symptoms of colitis, which contain weight loss, an occurrence of blood in a stool and stool consistency were measured daily. Experiments were performed

after receiving approval of the Institutional Animal Care and Use Committee of the Institute of Laboratory Animal Resources, Seoul National University.

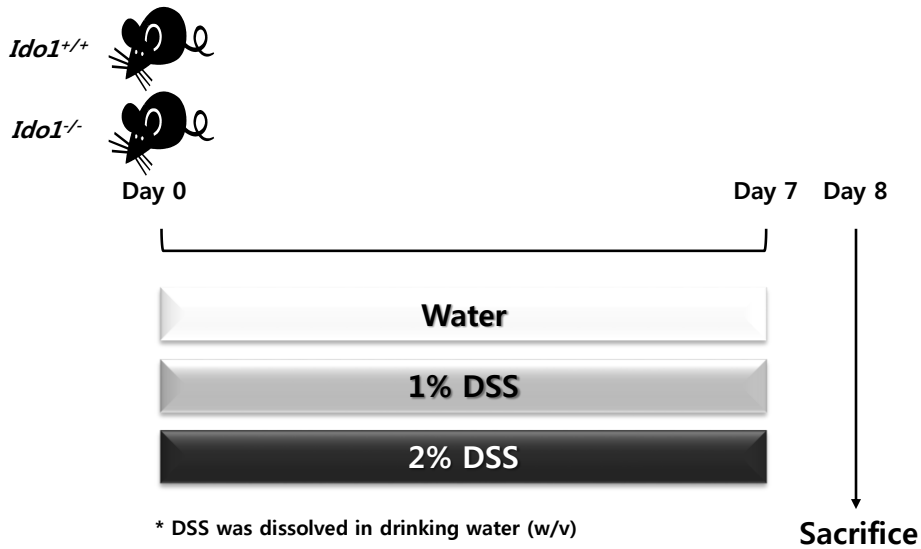

Figure 2. Experimental design for the DSS-induced colitis model.

Ido1$^{+/+}$ and *Ido1*$^{-/-}$ mice, which are 8–11 weeks of age, were divided into six groups (n=4–7 per group). DSS (1% or 2%) dissolved in drinking water (w/v) was given to mice for 7 days *ad libitum*. Weight loss, occurrence of blood in a stool, and stool consistency were measured daily. Mice were sacrificed at day 8, and colon tissues and intestinal contents were collected.

3. *Evaluation of development colitis*

In all mice, weight, stool consistence, and presence of stool blood were observed daily as previously described (Cooper, Murthy, Shah, & Sedergran, 1993).

The modified disease activity index (DAI) score was evaluated by grading on a 0 to 4 scale based on 3 parameters: change in weight (1, 5–10%; 2, 11–15%; 3, 16–20%; and 4, >21%), stool consistency (0, normal; 2, loose stools; 4, diarrhea), and stool blood (0, no blood seen; 2, obvious blood with stool; 4, grossly bloody stool). Percentage of body weight change was calculated as difference between the first bodyweight and the actual bodyweight on any particular day. It was calculated as formula:

$$\left[\text{body weight (day x)} - \textit{initial body weight (day 0)} \Big/ \textit{initial body weight (day 0)}\right] \times 100$$

Finally, an average of the three categories were calculated and specified in DAI score.

4. *Histology analysis*

At day 8, the end of the experiment, mice were sacrificed, and the large intestine contents were carefully removed with a forceps and snap-frozen in liquid nitrogen. For histological analysis, the middle part of a large intestine segment was rolled and fixed in formalin (Moolenbeek & Ruitenberg, 1981). In brief, the remaining bowel contents were removed with injecting PBS solution followed by open longitudinally with scissors. The tissue segment was rolled up like a "Swiss roll", fixed in formalin, stained with hematoxylin and eosin (H&E), and examined histologically. The histological scoring was determined using a previously described scoring method

(Kitajima, Takuma, & Morimoto, 2000; Laroui et al., 2012). The modified scoring criterion is detailed in **table 1.**

Table 1. Histological grading of colitis

Feature	Score	Description
Severity inflammation	0	Rare inflammatory cell in the lamina propria
	1	Increase inflammatory cell in the lamina propria
	2	Confluence inflammatory cell extending into the submucosa
	3	Transmural extension of the inflammatory infiltrate
Damage	0	None
	1	Loss of the basal 1/3 of the crypt
	2	Loss of the basal 2/3 of the crypt
	3	Loss of the entire crypt but intact epithelial cell
	4	Loss of the entire crypt and the surface epithelial cell
Extension	0	None
	1	Focal
	2	Lesion involving 1/3 of the intestine
	3	Lesion involving 2/3 of the intestine
	4	Lesion involving the entire intestine

5. *DNA extraction from large intestinal contents*

Total bacterial DNA was isolated from large intestinal contents by using the QIAamp® DNA stool Mini Kit (QIAGEN, Hilden, Germany) according to the kit protocol for pathogen detection with a few modifications. Briefly, an average of 110 mg intestinal contents were homogenized in ASL buffer using an IKA® T-10 Basic Ultra-Turrax homogenizer (IKA Werke GmbH & Co., Staufen, Germany) at power level 5.5 for one minute. Then, we heated the suspension at optional high-temperature step (95℃) to lyse gram positive bacterial cells. In last incubation step, we increased time from 1 min to 5 min to increase DNA yield. Extracted genomic DNA was quantified by spectrophotometer NanoDrop ND-2000 (Thermo Scientific, Waltham, MA, USA) and stored at -80 ℃ until use.

6. *Amplification of 16S rRNA gene and 454-pyrosequencing*

Hypervariable regions (V1－V3) of 16S rRNA gene were amplified using barcoded universal primers for each sample. Sample-specific barcoded primers for each sample are listed in **table 2.** Polymerase chain reaction (PCR) was carried out in a final volume of 50 $\mu\ell$ contained about 10 ng DNA template, 5 $\mu\ell$ of 10X Taq buffer(20mM Mg^{2+}), 1 $\mu\ell$ of 10 mM dNTP mix, 2 $\mu\ell$ of forward and reverse barcoded primers (20 pmol/$\mu\ell$), 2.5 U of Taq DNA polymerase (SolGent Co., Seoul, Korea). PCR reactions were amplified on a GeneAmp® PCR system 9700 (Applied Biosystems, Foster City, CA, USA). PCR program was as follows: initial for 5 min

hold at 94℃, followed by 30 cycles of denaturation (30 sec, 94℃), annealing (30 sec, 55℃), extension (30 sec, 72℃); with a final extension step of 7 min at 72℃ followed by holding at 4℃. The PCR product was confirmed by using 1% agarose gel electrophoresis and visualized under a Gel Doc system (BioRad, Hercules, CA, USA).

The amplified products were purified using the QIAquick PCR purification kit (Qiagen, Valencia, CA, USA), and purified PCR products (500ng) of each mouse were mixed. Pyrosequencing was performed using a 454 GS FLX Titanium platform (Roche, Mannheim, Germany), according to the manufacturer's instructions by Chunlab, Inc. (Seoul, Korea).

Table 2. List of adapter and fusion primer sequences used in this study

Name	Sequence (5'-3')
454 Adapter 1	CCATCTCATCCCTGCGTGTCTCCGAC
454 Adapter 2	CCTATCCCCTGTGTGCCTTGGCAGTC
Key sequence	TCAG
Fusion primer (barcoded primers)	
Forward[1]	
B16S-F	CCTATCCCCTGTGTGCCTTGGCAGTC-TCAG-AC-GAGTTTGATCMTGGCTCAG
Bif16S-F	CCTATCCCCTGTGTGCCTTGGCAGTC-TCAG-AC-GGGTTCGATTCTGGCTCAG
Reverse[2]	
B16-7-1	CCATCTCATCCCTGCGTGTCTCCGAC-TCAG-**TCGTCAT**-AC-WTTACCGCGGCTGCTGG
B16-7-4	CCATCTCATCCCTGCGTGTCTCCGAC-TCAG-**AGAGCTG**-AC-WTTACCGCGGCTGCTGG
B16-7-7	CCATCTCATCCCTGCGTGTCTCCGAC-TCAG-**TCAGATG**-AC-WTTACCGCGGCTGCTGG
B16-7-8	CCATCTCATCCCTGCGTGTCTCCGAC-TCAG-**CGATGAG**-AC-WTTACCGCGGCTGCTGG
B16-7-12	CCATCTCATCCCTGCGTGTCTCCGAC-TCAG-**TCTGCAG**-AC-WTTACCGCGGCTGCTGG
B16-7-13	CCATCTCATCCCTGCGTGTCTCCGAC-TCAG-**AGCGATG**-AC-WTTACCGCGGCTGCTGG
B16-8-3	CCATCTCATCCCTGCGTGTCTCCGAC-TCAG-**ATGCTGAG**-AC-WTTACCGCGGCTGCTGG
B16-8-4	CCATCTCATCCCTGCGTGTCTCCGAC-TCAG-**TACAGCAG**-AC-WTTACCGCGGCTGCTGG
B16-8-18	CCATCTCATCCCTGCGTGTCTCCGAC-TCAG-**ATCGTGTG**-AC-WTTACCGCGGCTGCTGG
B16-8-21	CCATCTCATCCCTGCGTGTCTCCGAC-TCAG-**CTACACAG**-AC-WTTACCGCGGCTGCTGG
B16-8-24	CCATCTCATCCCTGCGTGTCTCCGAC-TCAG-**TAGCTACG**-AC-WTTACCGCGGCTGCTGG
B16-8-27	CCATCTCATCCCTGCGTGTCTCCGAC-TCAG-**TCGAGTAG**-AC-WTTACCGCGGCTGCTGG
B16-9-4	CCATCTCATCCCTGCGTGTCTCCGAC-TCAG-**CGTGTACTG**-AC-WTTACCGCGGCTGCTGG

[1] Mixture of B16S-F and Bif16S-F (9:1 ratio) was used.

[2] Barcode sequences are shown in bold type.

7. *Pyrosequencing data analysis*

The change of microbial community composition was determined using Ribosomal Database Project (RDP) pyrosequencing pipeline (http://pyro.cme.msu.edu/; release 11) (Cole et al., 2014) at each phylogenetic level. Primer sequence, key tag, and the sequences of low quality (average score < 20) were removed using the initial processing step of the RDP. Any reads containing more than one 'N's (ambiguous nucleotides), and/or reads shorter than 300bp were also excluded from further analysis.

Chimeric sequences were excluded by UCHIME (Edgar, Haas, Clemente, Quince, & Knight, 2011) included in USEARCH ver. 6.0 and aligned. Chimera removed sequences classified by RDP-classifier (Wang, Garrity, Tiedje, & Cole, 2007) and rarefaction analysis was carried out by the RDP pipeline at a confidence threshold of 97%.

8. *Statistical Analysis*

Differences between the two groups were tested with unpaired *t*-test. A Linear regression analysis between severity of colitis and relative abundance of genus was carried out. All data were analyzed using GraphPad Prism v 5.0 (GraphPad Software, Inc., San Deigo, CA, USA).

III . Results

1. *Different disease severity between Ido1$^{+/+}$ and Ido1$^{-/-}$ mice*

As our preliminary experiments, we predicted that the inflammatory response may differ between *Ido1*$^{+/+}$ and *Ido1*$^{-/-}$ mice. So firstly, mice were chemically treated to induce colitis in order to see the difference in the inflammatory reaction. While the mice were developing colitis, body weight, fecal bleeding, and stool consistency were monitored daily. Those clinical symptoms of colitis began to be observed at day 5 after DSS treatment.

DSS-induced colitis was developed in *Ido1*$^{+/+}$ and *Ido1*$^{-/-}$ mice in a dose dependent manner, but *Ido1*$^{-/-}$ mice were significantly less susceptible to DSS treatment. At day 7, weight loss has occurred in both *Ido1*$^{+/+}$ and *Ido1*$^{-/-}$ group, -23.15±2.90% and -13.45±1.93%, respectively in 2% DSS-treatment groups (P=0.0495) **(Figure 3)**. There was also statistical difference in Disease Activity Index (DAI) score by genotype (P<0.05), too. No significant difference between *Ido1*$^{+/+}$ and *Ido1*$^{-/-}$ mice was observed in control (0%) and 1% DSS treatment group; however, *Ido1*$^{-/-}$ mice showed lower DAI scores than *Ido1*$^{+/+}$ mice **(Figure 4)**.

The shortening of colon length is another indicator of colitis development. As seen our data, colon length was significantly reduced in DSS-dose dependent manner. Strikingly, inflamed colon in 2% DSS-treated was significantly shorten in *Ido1*$^{+/+}$, compared to *Ido1*$^{-/-}$ mice (P=0.015) **(Figure 5 and 6)**. Histological analysis was performed to check histologic severity of inflammation, damage of crypt, and extension. *Ido1*$^{-/-}$ mice showed more intact mucosal barrier than *Ido1*$^{-/-}$ mice in 1%

DSS group **(Figure7)**. Colitis progressed too far, meaning that disease developed to the final stage in 2% DSS groups, we failed to detect the significant difference in histological scores between *Ido1*$^{+/+}$ and *Ido1*$^{-/-}$ mice **(Figure 8)**.

Together from the results above, it was found that *Ido1*$^{-/-}$ mice were less susceptible to DSS treatment during colitis development.

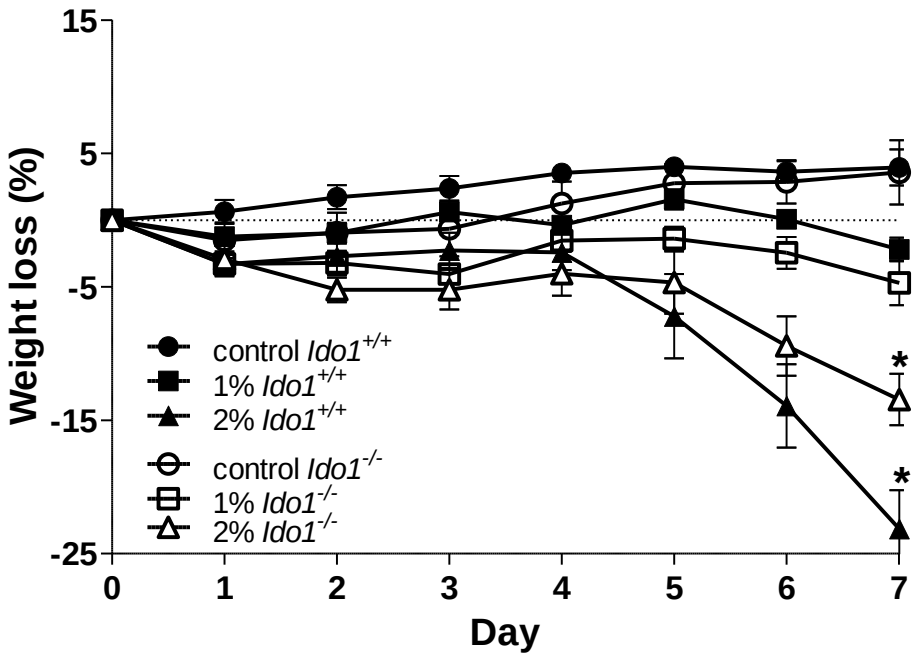

Figure 3. Percentage body weight changes during colitis development

Percentage body weight changes of *Ido1*$^{+/+}$ and *Ido1*$^{-/-}$ mice supplied 0%, 1%, and 2% DSS (w/v) water for 7 days were measured. Weight (g) was measured daily, and percentages of body weight changes were calculated by the percent weight change relative to the initial weight. Data are presented as means ± SEM (n = 3–5 per group) and *p*-value was estimated by unpaired *t*-test. The asterisks denote significant differences at $P < 0.05$.

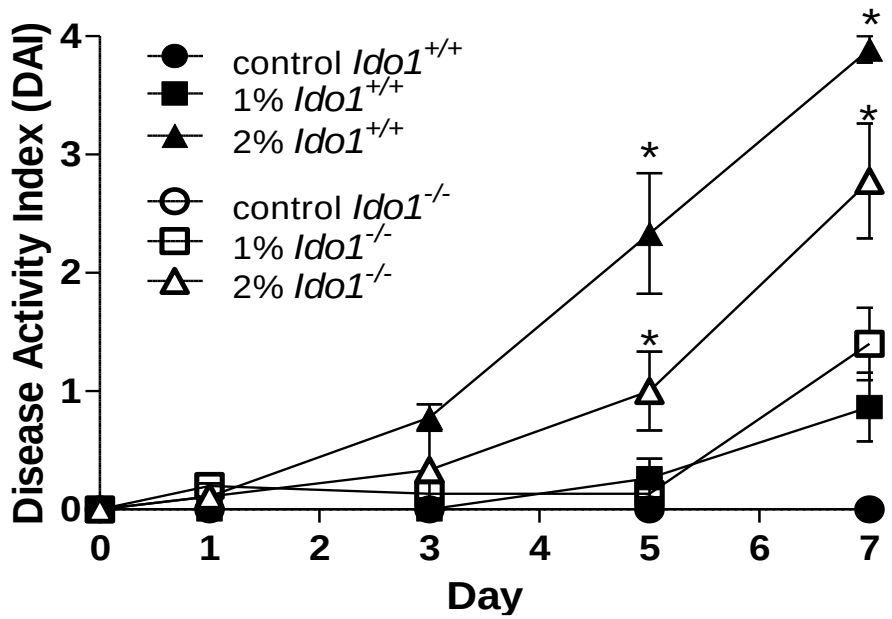

Figure 4 . Disease activity index (range from 0–4, maximal score) displaying the course of colitis induction

Disease activity index is described by percentage of body weight loss (0–4, depending on % of body weight change), stool consistency (0, normal; 2, loose stools; 4, diarrhea), and fecal bleeding (0, no blood seen; 2, obvious blood with stool; 4, grossly bloody stool). The average score of parameters is shown. Data are presented as means ± SEM (n = 3–5 per group), and *p*-value was estimated by unpaired *t*-test. The asterisks denote significant differences at $P < 0.05$.

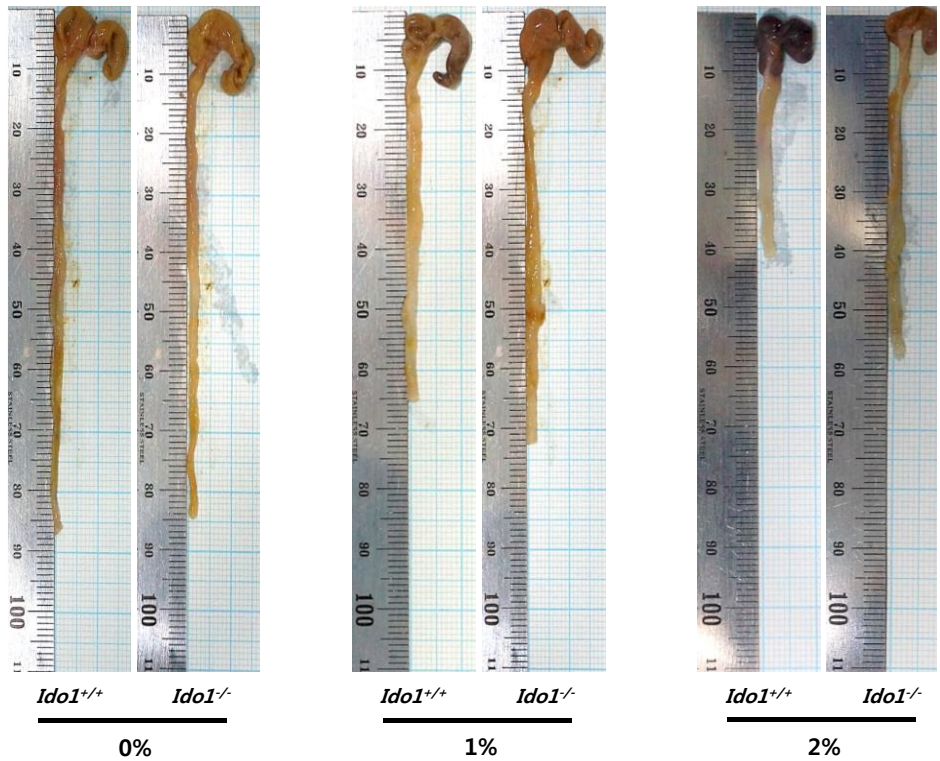

Figure 5. Colon length on the last day of DSS-treatment

Ido1$^{-/-}$ mice and *Ido1*$^{+/+}$ mice were treated with 0%, 1%, or 2% DSS (w/v) water for 7 days. At day 8, mice were sacrificed and the entire colon was removed. The colon length from post-cecum to anus was measured. Representative images for each group are shown. Numbers in the bottom are in mm.

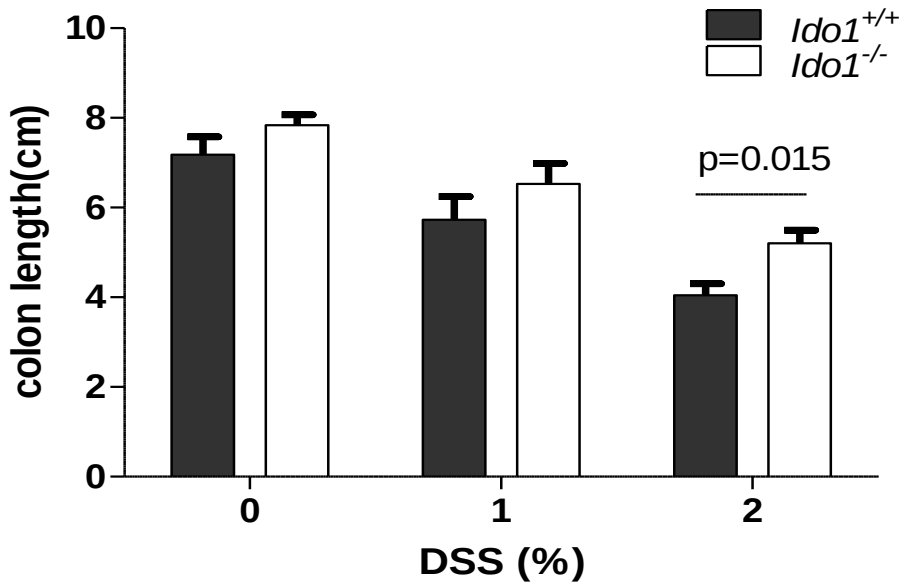

Figure 6. Entire colon length

Ido1$^{-/-}$ mice and *Ido1*$^{+/+}$ mice were treated with 0%, 1%, or 2% DSS (w/v) water for 7 days. At day 8, mice were sacrificed, and entire colons were removed. Entire colon lengths (except cecum) were measured by ruler. Bar graphs represent means ± SEM (n=3–6 for each groups), and *p*-values were estimated by unpaired t-test.

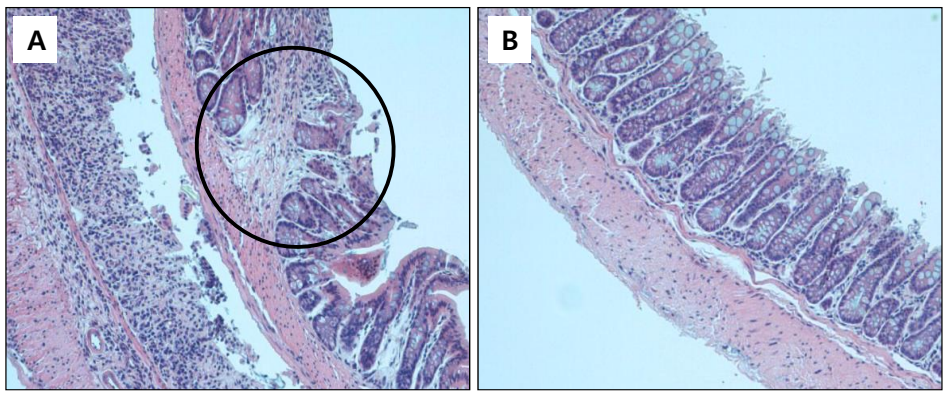

Figure 7. Histology of colonic tissue sections (hematoxylin-eosin, X 200)
Following sacrifice, the middle parts of colons were stained with hematoxylin-eosin for histological examination. Representative images for the 1% DSS–treated group are shown. Panels A and B are representative images of *Ido1*$^{+/+}$ and *Ido1*$^{-/-}$ mice in the 1% DSS group, respectively. Disrupted mucosa layers are presented in circle in panel A. Specimens were observed by Olympus BX50 microscope and PAXcam_microscope software.

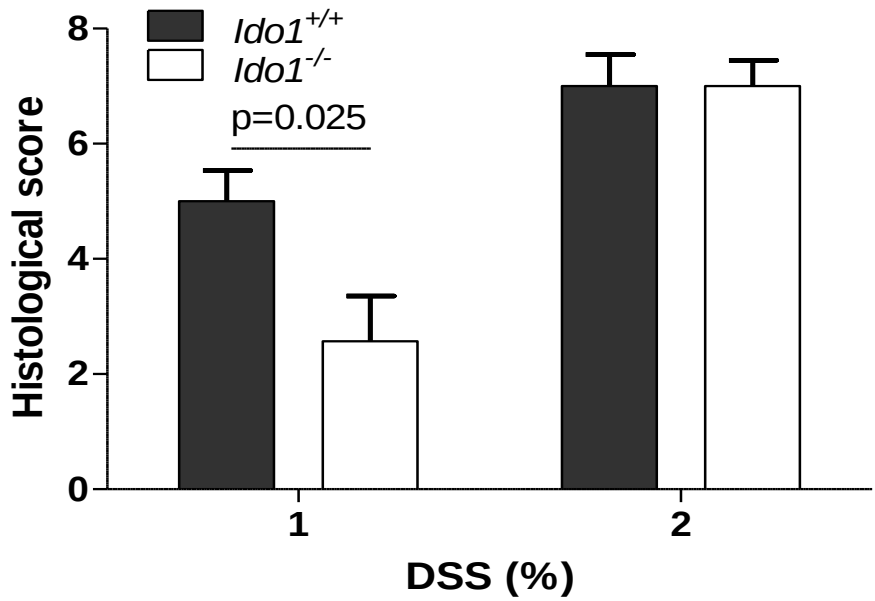

Figure 8. Histological sores of hematoxylin-eosin stained colons

Following sacrifice, the middle parts of colons were stained with hematoxylin-eosin for histological examination. Histological score is calculated by the sum of severity of inflammation (0–3), damage (0–4), and extension (0–4). Bar graphs represent means ± SEM (n = 5–7 per group) of samples within a group, and *p*-value was estimated by unpaired *t*-test.

2. *Pyrosequencing of 16S rRNA genes for microbial community analysis*

To investigate the composition of gut flora in each group, pyrosequencing was performed. Twenty three large intestinal contents were randomly selected from the six groups of mice (*Ido1*$^{+/+}$+0% DSS, n=3; *Ido1*$^{+/+}$+1% DSS, n=5; *Ido1*$^{+/+}$+2% DSS, n=4; *Ido1*$^{-/-}$+0% DSS, n=3; *Ido1*$^{-/-}$+1% DSS, n=4; *Ido1*$^{-/-}$+2% DSS, n=4). The 16S rRNA gene from each sample was sequenced, after they were amplified with barcoded PCR primers from genomic DNA extracted from large intestinal contents. After trimming the barcodes, chimeras and low quality reads were removed using Ribosomal Database Project (RDP) pipeline and UCHIME. As can be seen in Figure 9, 4,204 to 7,354 valid sequences were obtained and average number of sequences were about 5300 per sample **(Figure 9)**. The number of valid sequences were not significantly different among six groups (data not shown).

Valid sequences were clustered into operational taxonomic units (OTUs) at the 97% similarity cut-off, which is typically the species level. OTU-based rarefaction curves reached flat, showing that depth of sequencing would reasonably well describe our microbial communities **(Figure 10)**.

To see how microbial communities were changed in disease progression, relative abundances of phyla were calculated. When colitis was severe, *Ido1*$^{+/+}$ mice had one or two bacteria which accounted for more than 90% of the total, whereas the *Ido1*$^{-/-}$ group still had a various type of phylum. These data showed that *Ido1*$^{-/-}$ mice had significantly more diversity than *Ido1*$^{+/+}$ mice. **(Figure 11)**.

Complexities in the composition of gut microbiota decreased in mice with severe colitis. These results have accordance with our findings that *Ido1*$^{+/+}$ mice developed more severe colitis compared with *Ido1*$^{-/-}$ mice.

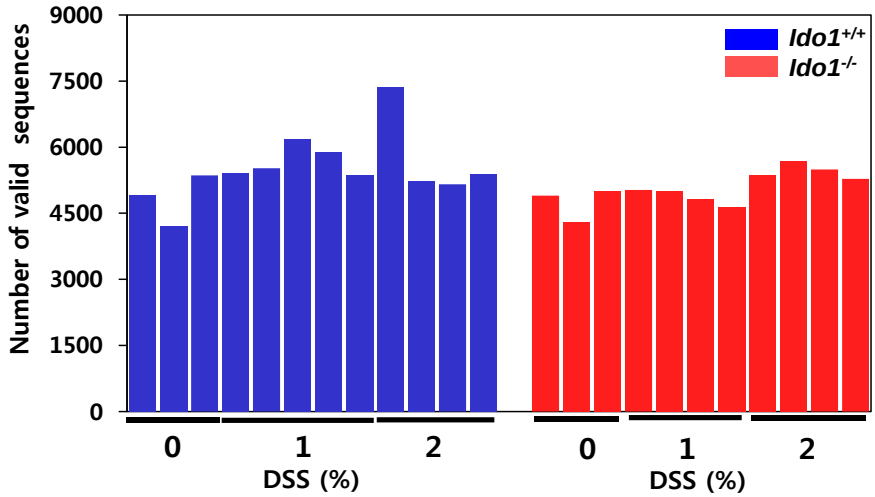

Figure 9. Number of valid sequences per group

The number of valid sequences that have trimmed-out barcode, chimeras, and low quality reads are shown. The bars represent the number of valid sequences of each sample (n=3-5 per group). The blue bar and red bar present *Ido1*$^{+/+}$ and *Ido1*$^{-/-}$, respectively.

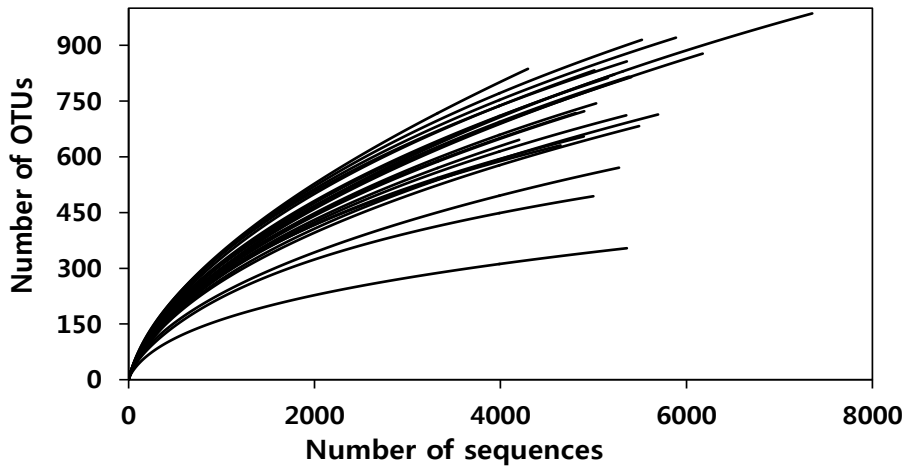

Figure 10. Plot of rarefaction curves

The numbers of operational taxonomic units (OTUs) are defined by 0.03-distance cut-off. The x-axis and y-axis present the number of valid sequences and the number of OTUs, respectively. Curves represent each sample (n = 3−5 per group).

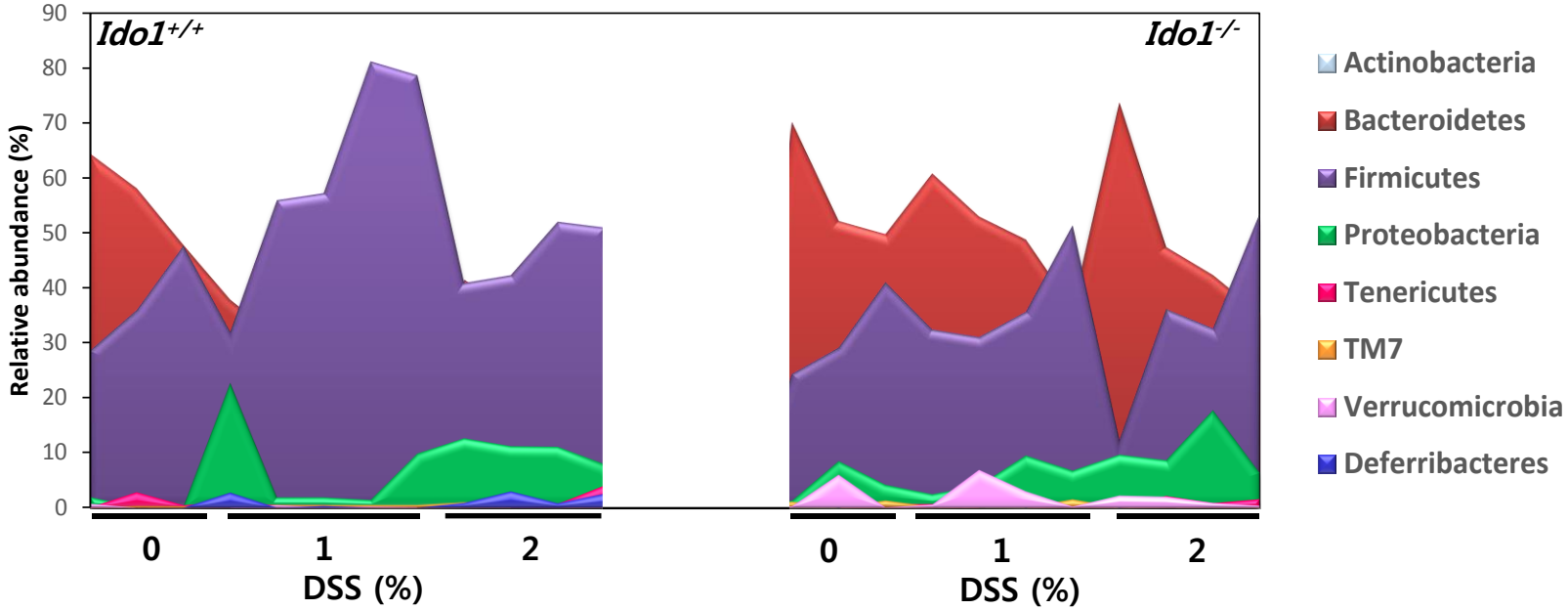

Figure 11. Relative abundance of intestinal bacterial phyla

Pyrosequencing was performed using 23 representative samples from six groups of mice (n = 3–5 per group). Collected sequences of samples were subsequently analyzed and classified by phylum. Eight phyla were identified, and shown by genotype and DSS concentration.

3. *Ratios of Bacteroidetes to Firmicutes*

According to our hypothesis, the composition of intestinal microbiota might be different depending on whether the host can use tryptophan or not. To test the hypothesis, we examined the difference of microbiome profiles between *Ido1*$^{+/+}$ and *Ido1*$^{-/-}$ mice. Our data showed that the predominant phyla were Bacteroidetes, Firmicutes, Proteobacteria, Tenericutes, TM7, Deferribacteres, Verrucomicrobia, and Actinobacteria. Moreover, Bacteroidetes, Firmicutes, and Proteobacteria were the three most abundant phyla in all groups. The relative abundance of Proteobacteria increased, when the severity of colitis progressed. In the case of *Ido1*$^{+/+}$—not in *Ido1*$^{-/-}$—mice, Deferribacteres showed up after colitis induction. In contrast, Verrucomicrobia only existed in *Ido1*$^{-/-}$ mice **(Figure 11)**.

Predominant phyla classified into two categories; gram-positive and gram-negative bacteria. Bacteroidetes, Deferribacteres, Proteobacteria, Tenericutes, and Verrucomicrobia belong to gram-negative while others are gram-positive. As seen in Figure 12, unlike *Ido1*$^{+/+}$, gram-negative were nearly 1.8-fold more than gram positive bacteria at any dose in *Ido1*$^{-/-}$. Gram-positive and negative bacteria reflected two most represented phyla, Firmicutes and Bacteroidetes, respectively. So, these phyla were further analyzed in detail.

Figure 13 showed the association of relative abundance of the two phyla. Linear regression analysis showed that there was a significant negative correlation between Firmicutes and Bacteroidetes (P<0.001) and goodness of the fit was R^2=0.8355. Relative abundance of bacteria at phylum level indicated that Firmicutes were the

most predominant in inflamed *Ido1*$^{+/+}$ colon, but Bacteroidetes was the most prevalent one in *Ido1*$^{-/-}$ mice **(Figure 13)**.

Interestingly, ratio of Bacteroidetes to Firmicutes was dramatically reduced in DSS treated *Ido1*$^{+/+}$ colon (1.62 to 0.76), however, the ratio got increased in *Ido1*$^{-/-}$ colitis mice (1.96 to 2.31). Ratios of Bacteroidetes to Firmicutes in *Ido1*$^{-/-}$ were always higher than those in *Ido1*$^{+/+}$ at any dose; the difference in the ratio between *Ido1*$^{+/+}$ and *Ido1*$^{-/-}$ was enlarged in severe colitis model **(Figure 14)**.

In summary, compared to *Ido1*$^{-/-}$ mice, *Ido1*$^{+/+}$ mice showed less complex bacteria flora and they had more Firmicutes than Bacteroidetes in their inflamed colon.

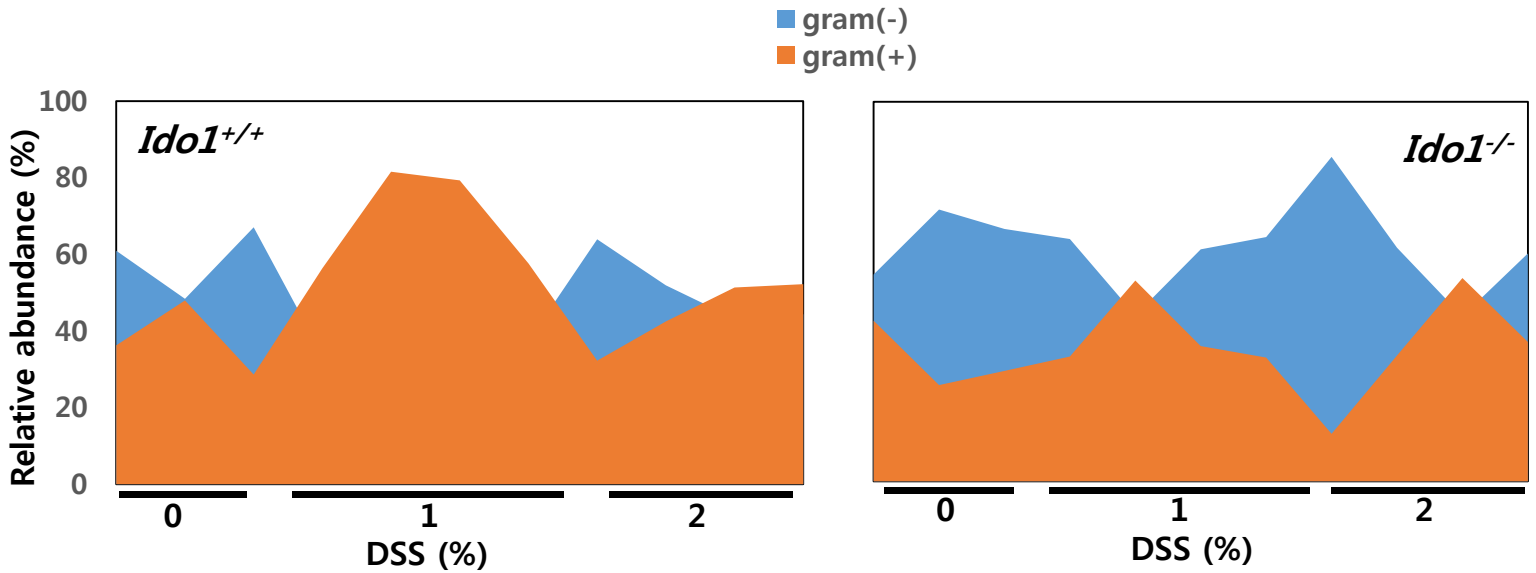

Figure 12. Different distributions of Gram-positive and Gram-negative bacteria in the *Ido1*$^{+/+}$ and *Ido1*$^{-/-}$ groups

The eight phyla are divided into gram-positive and gram-negative (three Gram-positive and five Gram-negative). Orange and blue graphs present gram-positive and negative, respectively. Relative abundance of individual mice (n = 3–5 per group) are shown by genotype and DSS concentration.

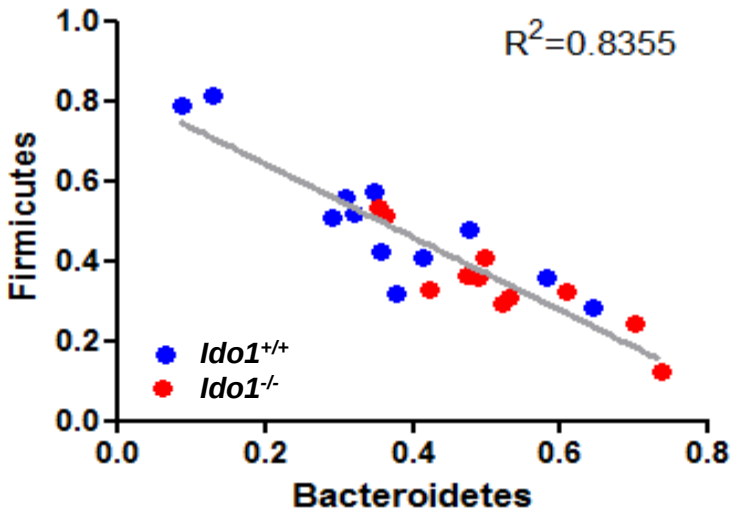

Figure 13. Association of relative abundance of Bacteroidetes and Firmicutes.

Regression equation by linear regression analysis; each dot represents an individual mouse (n=23). Blue dots and red dots indicate *Ido1*$^{+/+}$ and *Ido1*$^{-/-}$, respectively. Linear regression and R-square are indicated for each region.

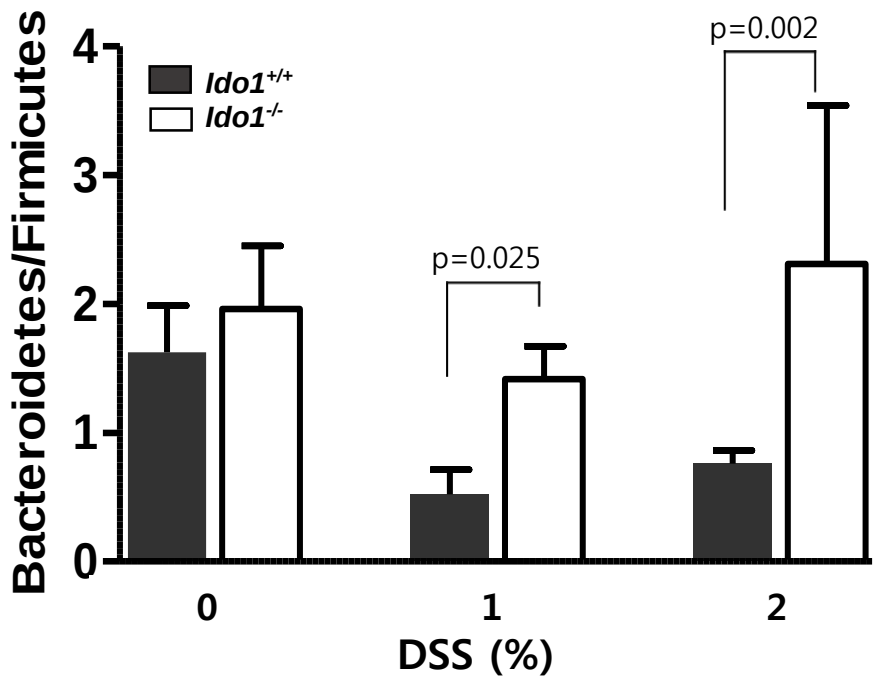

Figure 14. The pattern of Bacteroidetes/Firmicutes ratio

The patterns of change in Bacteroidetes/Firmicutes ratio in the intestinal microbiota of *Ido1*$^{+/+}$ and *Ido1*$^{-/-}$ mice by dose dependent manner were analyzed. Black and white bars indicate *Ido1*$^{+/+}$ and *Ido1*$^{-/-}$ mice, respectively. All data represent means ± SEM of samples within a group (n = 3–5 per group), and *p*-values were determined by unpaired *t*-test.

4. *Commensal bacteria, depending on the absence of host's tryptophan metabolism*

As mentioned in previous section, profiles of gut microbiota was dramatically different at phylum level according to host's genotype and DSS concentration. However, the question what specific kinds of bacteria made the difference was not answered yet. To investigate further distinctions in a more specific type of bacteria, and next we focused on genus level.

To begin with, PCA was carried out to confirm if bacterial community were distinguished one from another successfully or not. Figure 15 illustrated the PCA of profiles of the colonic microbiota based on genera. As expected, due to the severity of disease specificity, a clear distinctions were observed among DSS concentration. Interestingly, not only the distinctions were based on disease severity, but also were based on host's genotype **(Figure 15)**.

Data were classified down to genus level through the RDP pipeline; consequently, total 57 types were identified. Differentially expressed genera were identified using ANOVA and they were selected based upon their *P*-value of less than 0.1. *Bacteroides, Parabacteroides, Barnesiella, Prevotella, Coprobacilius, Turicibacter, Hydrogenoanaerobacterium, Butyricicoccus, Lachnospiracea_incert ae_sedis, Robinsoniella, Mucispirillum, Marvinbryantia, Anaerotruncus* turned out to be the most significant genera that were affected by existence of *Ido1*. Especially, *Bacteroides, Parabacteroides, Barnesiella, Prevotella* were recognized as the significant five genera in *Ido1*$^{-/-}$ mice. These four genera showed significantly more

distributed at 0% DSS in *Ido1*$^{-/-}$ mice (P<0.05). This trend has continued in the 1% DSS group, but different in 2% DSS group **(Figure 16)**.

For example, *Bacteroides* was higher more than 30-fold in *Ido1*$^{-/-}$ compared to *Ido1*$^{+/+}$ at any dose. And the difference was shown a greater in 2% DSS-treated mice in particular. The *Ido1*$^{-/-}$ group treated 2% DSS; *Bacteroides* tended significantly 9.21×10^{8}-fold higher than *Ido1*$^{+/+}$. Interestingly, three of the four—*Bacteroides, Parabacteroides, and Prevotella*—are known as bacteria to produce indole by tryptophan metabolism (Lee & Lee, 2010; Russell et al., 2013; Yokoyama & Carlson, 1979). This implies that tryptophan remained in gastrointestinal (GI) tract of *Ido1*$^{-/-}$ mice could be used by those bacteria that are able to utilize tryptophan in their environment.

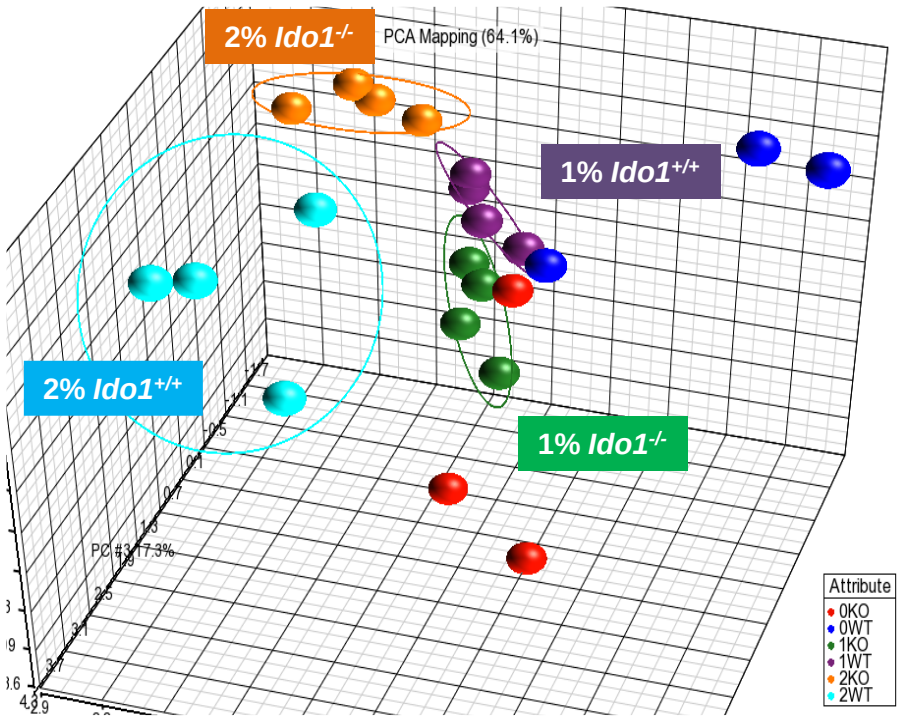

Figure 15. Principle component analysis (PCA)

Intestinal bacteria were analyzed at genus level. The results are depicted 3-dimensionally as the X, Y, and Z axes. Each color dot represents data from an individual animal (n = 3 or 4 per group), and multiple dots from the same group are shown as large circles.

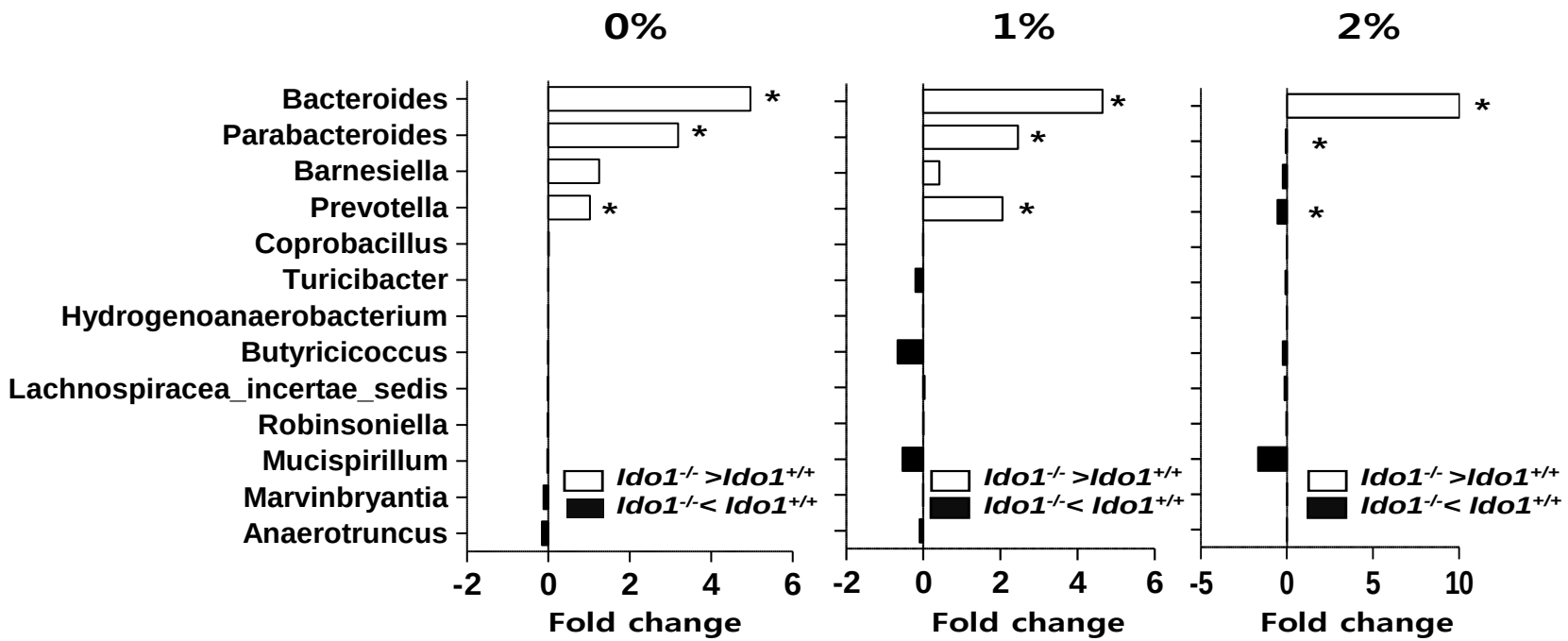

Figure 16. Average fold change of 13 genera in *Ido1*$^{+/+}$ compared with *Ido1*$^{-/-}$ mice

Bar graphs summarize the top 13 most differentially expressed genes between *Ido1*$^{+/+}$ (■) and *Ido1*$^{-/-}$ (□) mice in three doses. Results are depicted as relative fold change, where negative values are more highly expressed in the *Ido1*$^{+/+}$ mice, and positive values are more highly expressed in the *Ido1*$^{-/-}$ mice. Asterisks refer to indole producing genera

5. *Commensal bacteria, depending on the severity of the disease*

Finally, we decided to take a look at the correlation between the relative abundance of the genus and the severity of disease that includes % weight change, DAI, and histology evaluation. At first, we have selected the bacteria, which are different patterns between 0% DSS and 2% DSS in *Ido1*$^{+/+}$ mice (t-test, p<0.1). *Oscillibacter, Turicibacter, Paraprevotella, Mucispirillum, and Escherichia/shigella* turned out to be the most significant genera that were affected by disease progression. However, as shown in figure 17, this tendency in *Ido1*$^{+/+}$ mice not correspond to *Ido1*$^{-/-}$ mice. As the condition of severe colitis model (2% DSS), *Oscillibacter* and *Turicibacter* were increased regardless of genotype. Meanwhile, *Paraprevotella, Mucispirillum, and Escherichia/shigella* had risen only in *Ido1*$^{+/+}$ mice **(Figure 17)**.

After five genera—which related to disease severity—were selected, these were further analyzed to learn more about the link between indicators of the seriousness of colitis. Percentage of body weight change and histological scoring were used.

First, correlation between five genera and percentage of body weight change was reported in Figure 18. Slope from linear regression analysis was significantly positive in the correlation between loss of body weight and *Oscillibacter* (P=0.032, R^2=0.2000), *Turicibacter* (P=0.004, R^2=0.3385) in both *Ido1*$^{+/+}$ and *Ido1*$^{-/-}$ mice **(Figure 18)**. In the case of histological score, same results were observed **(Figure 19)**. That were, *Oscillibacter* (P=0.009, R^2=0.2815) and *Turicibacter* (P=0.001, R^2=0.2778) which had positive relations with histology scores.

When the disease becomes serious; *Paraprevotella*, *Mucispirillum*, and *Escherichia / Shigella* were significantly higher in *Ido1*$^{+/+}$ than *Ido1*$^{-/-}$, and these three genera were increased a weight loss dependently in *Ido1*$^{+/+}$ **(Figure 18 and 19)**. Interestingly, *Paraprevotella* (P=0.014, R^2=0.4667) and *Mucispirillum* (P=0.018, R^2=0.4419) were exclusively positive correlated between loss of body weight in *Ido1*$^{+/+}$ mice.

In the case of histological score, three genera were not significantly positive linear correlated. But there were same patterns between histological score and relative abundance of three genera as seen previously. When the disease became serious; *Paraprevotella* (P=0.157, R^2=0.1894), *Mucispirillum* (P=0.060, R^2=0.3104), and *Escherichia / Shigella* (P=0.0723, R^2=0.2875) were higher in *Ido1*$^{+/+}$ than in *Ido1*$^{-/-}$ mice **(Figure 19).** It may be inferred that three genera have a role in aggravation of colitis in mice.

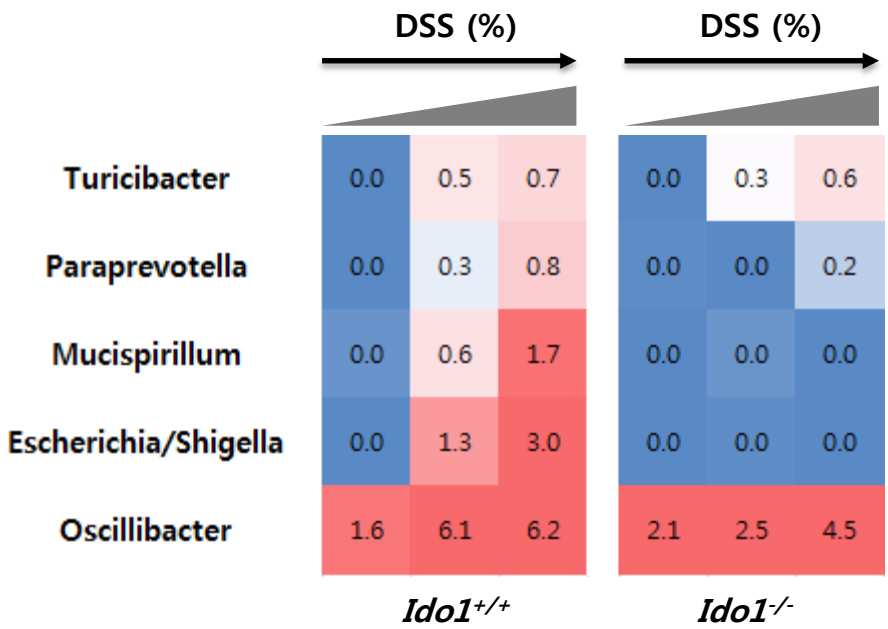

Figure 17. Five genera in relationship with disease progression

Five genera were identified by t-test between DSS 2% vs. 0% in wild-type mice. Values were average percentages of 3–5 mice per group.

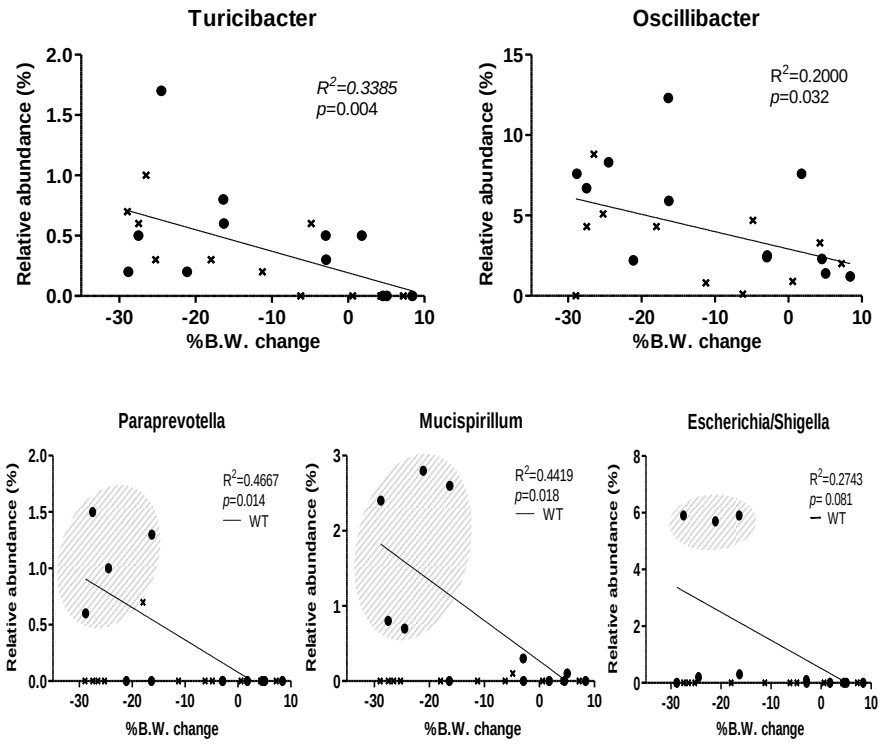

Figure 18. Relation between body weight change and relative abundance of genera

Weight (g) was measured daily, and percentages of body weight changes were calculated relative to the initial weight. The graph showed changes in percentage body weight change of individual mice on day 7 (n=23). Weight loss increases as it goes from right to left on the x-axis. Linear regression, R-square, and p-value are indicated for each region.

●: *Ido1*$^{+/+}$ mice

X: *Ido1*$^{-/-}$ mice

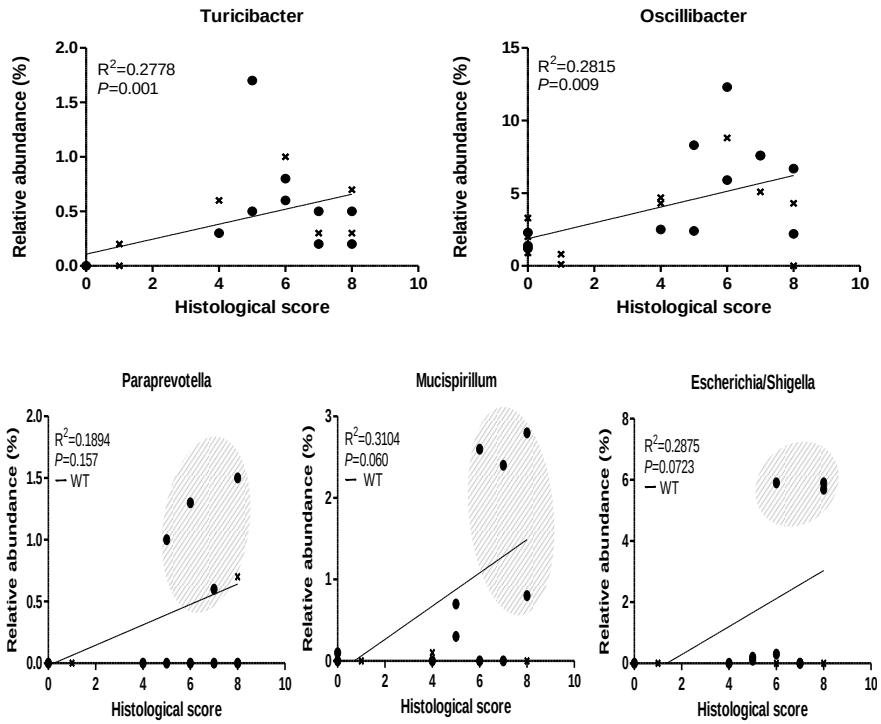

Figure 19. Relation between a histological score and relative abundance of genera

Following sacrifice, the middle parts of colons were stained with hematoxylin-eosin for histological examination. Histological score is calculated by sum of severity inflammation (0–3), damage (0–4), and extension (0–4) in individual mice (n = 23). The histological score increases as it goes from left to right on the x-axis. Linear regression, R-square, and *p*-value are indicated for each region.

●: *Ido1*$^{+/+}$ mice

X: *Ido1*$^{-/-}$ mice

IV . Discussion

The objective of this study was to test the hypothesis that tryptophan metabolism mediates the association between intestinal commensal bacteria and host inflammatory responses. In the past, many researchers have focused on the harmful effects of bacteria as a pathogen. However, recent research on commensal bacteria's symbiotic relationship with a host has expanded to its physiologically and immunologically beneficial roles. In particular, it became possible to obtain detailed information about many environmental bacteria that had not been cultured, through Next-Generation Sequencing (NGS) technology (Mardis, 2008).

The only difference is the environment in which the mice have grown up, as can be seen in our results, their expression of *Ido1* has changed. These findings prompted us to study the interaction between intestinal commensal bacteria and host tryptophan metabolism using *Ido1*-deficient mouse. Therefore, this study focused on how the metabolic enzymes of tryptophan, *Ido1*, and dependent-gut flora affect the phenotype of the disease using a metagenomic approach.

Gurtner et al. have illustrated that the expression of *Ido1* is remarkably increased from the basal level in TNBS colitis, a Th1-mediated disease. Moreover, the inhibition of *Ido1* in this setting augments the Th1 inflammatory response associated with this colitis model (Gurtner, Newberry, Schloemann, McDonald, & Stenson, 2003). Because *Ido1* has the anti-inflammatory roles, we predicted that if mice had no *Ido1*, diseases would have a bad effect.

However, when viewing many of the elements that reflect the severity of a disease, this study shows that *Ido1*$^{+/+}$ induced a more severe disease than *Ido1*$^{-/-}$ mice with DSS colitis. The difference between such results may come from the differences in the mechanisms of the chemicals that cause the disease. The mechanism of the DSS model considers that the infiltration of commensal bacteria due to the destruction of intestinal epithelial cells (IECs) is caused directly by the chemical, and is not a T-cell-dependent cause (Johansson et al., 2010; Rakoff-Nahoum, Paglino, Eslami-Varzaneh, Edberg, & Medzhitov, 2004). It is a limitation that this study cannot know the T-cell-mediated cause of the disease, but it is a better approach to observe the associations with the gut microbiota. For that reason, in this study, the composition of bacteria that changed when the disease was induced had a significant impact on the disease.

First, we found that *Ido1*$^{-/-}$ mice had significantly more diversity than *Ido1*$^{+/+}$ mice at the phylum level. Our results are accordance with earlier studies, which showed that the diversity in gut microbial composition was reduced in patients with IBD (Ott et al., 2004). Therefore, the composition of gut microbiota was decreased in severe colitis mice, and these results are in accordance with disease severity, which showed that *Ido1*$^{+/+}$ mice had more severe colitis than *Ido1*$^{-/-}$ mice.

Another interesting result in this study is the ratios of Bacteroidetes to Firmicutes. *Ido1*$^{-/-}$ mice were always higher than those in *Ido1*$^{+/+}$ at any dose, and the difference in the ratio between *Ido1*$^{+/+}$ and *Ido1*$^{-/-}$ was enlarged in the severe colitis model. Much research has shown a lower ratio of Bacteroidetes

to Firmicutes in patients with obesity. The case of IBD has not yet been wholly investigated, but it may increase the ratio of Bacteroidetes to Firmicutes (Clemente, Ursell, Parfrey, & Knight, 2012). Our results may another evidence for ratio of two phyla in DSS-induced colitis.

The gut microbiome, which was altered specifically in *Ido1*-deficient mice, synthesized indole from tryptophan. Recently, an important discovery was made involving the inter-kingdom signaling between commensal bacteria and the host cells in the GI tract. It is considered to be an important mediator of homeostasis and disease through intra-kingdom (i.e., recognition of bacterial signals by other bacteria) and/or inter-kingdom (i.e., recognition of host signals by bacteria and vice-versa) communication (Bansal, Alaniz, Wood, & Jayaraman, 2010). Among the bacterial signal molecules, indole has recently received much attention, due to its diverse biological roles in several bacterial strains.

In a previous study, Zelate et al. showed that in *Ido1*-deficient mouse, *Lactobacilli* utilize tryptophan and convert to its metabolites, indole-3-aldehyde (IAld), followed by recognition in innate lymphoid cells (ILCs) by the aryl hydrocarbon receptor (AhR). AhR-dependent-IL-22 transcription is up-regulated, followed by stimulating the epithelial cells to produce antimicrobial proteins. As a result, the host receives the protection of inflammation and colonization of *Candida albicans* (Zelante et al., 2013). However, we have not demonstrated the differences between *Lactobacilli* based on hosts, particularly by genotype. Instead of *Lactobacilli*, we successfully isolated several specific

bacteria genera such as *Bacteroides*, *Parabacteroides*, and *Prevotella*. These three genera are also capable of producing indole, using its known tryptophan (Lee & Lee, 2010; Russell et al., 2013; Yokoyama & Carlson, 1979). These findings may explain how the causes of the disease are different, based on only the metabolic deficiency of the host. It seems to help relieve the disease through the indole produced by bacteria to inhibit the inflammatory cytokine, enhancing the expression of proteins involved in the tight junction (Bansal et al., 2010; Shimada et al., 2013). However, this is just literature evidence, and this study is unable to prove that by experiment. Therefore, further study is needed.

Moreover, in the present study, bacteria that have a protective role are more prevalent in *Ido1*$^{-/-}$ mice. For example, as Chil-sung Kang et al. demonstrated, *Akkermansia*-derived extracellular vesicles (EV) may have a protective effect against colitis. It can be assumed that *Akkermansia*— *Ido1*$^{-/-}$ specific bacteria (data not shown)—play an anti-inflammatory role in DSS-induced colitis (Kang et al., 2013).

Our study showed that *Escherichia/Shigella*, *Mucispirillum*, and *Paraprevotella* occupy a large area in *Ido1*$^{+/+}$ mice. *Escherichia/Shigella*, the pro-inflammatory bacteria, were only present in the *Ido1*$^{+/+}$mice, which is a result that corresponds to a results from IBD patients (Thorkildsen et al., 2013). Interestingly, the mucin degradader *Mucispirillum* was also at a high percentage, specifically only in *Ido1*$^{+/+}$ mice (Berry et al., 2012; Robertson et al., 2005). We postulate that the intestinal mucus layer was rapidly destroyed by the increase of mucin-degradable bacteria.

In regards to the permeability parameters of the colon, such as Zonula occludens-1 (ZO-1), proglucagon, and the transepithelial resistance and abundance of *Oscillibacter*, a negative correlation was reported. In our study, this genus showed a trend in the high *Ido1*$^{+/+}$ and *Ido1*$^{-/-}$ mice for disease progression (Lam et al., 2012). Overall, we can interpret the cause of severe colitis compared to *Ido1*$^{-/-}$ as follows. It is possible to assume that the disease is seriously induced in *Ido1*$^{+/+}$ mice through the cooperation of DSS and a function of the bacteria described above.

However, our study has some limitations for the taxonomic classification analyzed at the genus level. A particular species and a larger sample should be investigated. Further study should be performed using *Ido1*$^{-/-}$ mouse–associated bacteria, such as *Bacteroides, Parabacteroides,* and *Prevotella*. Such study is necessary for observing the expression of the permeability parameters of the colon due to the indolic compounds produced by tryptophan. In addition, *Akkermansia* may have a protective effect in *Ido1*$^{-/-}$ mice. However, there has been no investigation of amino acid metabolism by *Akkermansia*. Further study will lead to a better understanding of the amino acid metabolism of tryptophan, in particular.

In summary, this study concluded that the absence of tryptophan metabolism in the host could change the composition of gut microbiota, and altered gut microbiota may lead to a decrease in symptoms of DSS-induced colitis. Due to the lack of tryptophan metabolism in the host, tryptophan was relatively abundant in the large intestine; consequently, the *Bacteroides, Parabacteroides*,

and *Prevotella* that metabolize tryptophan to indole compounds increased. In *Ido1*$^{+/+}$ mice, *Mucispirillum*, which utilizes mucin and *Escherichia/Shigella*, which is well known as a pathogenic bacteria, was particularly high. Overall, these results suggest that *Ido1* plays roles in development of mouse IBD through alteration of intestinal commensal bacteria profiles. Our findings provide one of the evidences that host system intestinal microbiota may communicate by sharing nutrient metabolism networks.

V . References

Allegretti, J. R., & Hamilton, M. J. (2014). Restoring the gut microbiome for the treatment of inflammatory bowel diseases. *World Journal of Gastroenterology, 20*(13), 3468-3474. doi: 10.3748/wjg.v20.i13.3468

Archambaud, C., Sismeiro, O., Toedling, J., Soubigou, G., Bécavin, C., Lechat, P., . . . Cossart, P. (2013). The Intestinal Microbiota Interferes with the microRNA Response upon Oral Listeria Infection. *mBio, 4*(6), e00707-00713.

Backhed, F., Ley, R. E., Sonnenburg, J. L., Peterson, D. A., & Gordon, J. I. (2005). Host-bacterial mutualism in the human intestine. *Science, 307*(5717), 1915-1920. doi: 10.1126/science.1104816

Bansal, T., Alaniz, R. C., Wood, T. K., & Jayaraman, A. (2010). The bacterial signal indole increases epithelial-cell tight-junction resistance and attenuates indicators of inflammation. *Proceedings of the National Academy of Sciences, 107*(1), 228-233. doi: 10.1073/pnas.0906112107

Berry, D., Schwab, C., Milinovich, G., Reichert, J., Ben Mahfoudh, K., Decker, T., . . . Loy, A. (2012). Phylotype-level 16S rRNA analysis reveals new bacterial indicators of health state in acute murine colitis. *Isme j, 6*(11), 2091-2106. doi: 10.1038/ismej.2012.39

Cani, P. D., Bibiloni, R., Knauf, C., Neyrinck, A. M., Neyrinck, A. M., Delzenne, N. M., & Burcelin, R. (2008). Changes in gut microbiota control metabolic endotoxemia-induced inflammation in high-fat diet-induced obesity and diabetes in mice. *Diabetes, 57*(6), 1470-1481. doi: 10.2337/db07-1403

Clemente, Jose C., Ursell, Luke K., Parfrey, Laura W., & Knight, R. (2012). The Impact of the Gut Microbiota on Human Health: An Integrative View. *Cell, 148*(6), 1258-1270. doi: http://dx.doi.org/10.1016/j.cell.2012.01.035

Cole, J. R., Wang, Q., Fish, J. A., Chai, B., McGarrell, D. M., Sun, Y., . . . Tiedje, J. M. (2014). Ribosomal Database Project: data and tools for high throughput

rRNA analysis. *Nucleic Acids Res, 42*(Database issue), D633-642. doi: 10.1093/nar/gkt1244

Cooper, H. S., Murthy, S. N., Shah, R. S., & Sedergran, D. J. (1993). Clinicopathologic study of dextran sulfate sodium experimental murine colitis. *Lab Invest, 69*(2), 238-249.

Edgar, R. C., Haas, B. J., Clemente, J. C., Quince, C., & Knight, R. (2011). UCHIME improves sensitivity and speed of chimera detection. *Bioinformatics, 27*(16), 2194-2200.

Gill, S. R., Pop, M., Deboy, R. T., Eckburg, P. B., Turnbaugh, P. J., Samuel, B. S., . . . Nelson, K. E. (2006). Metagenomic analysis of the human distal gut microbiome. *Science, 312*(5778), 1355-1359. doi: 10.1126/science.1124234

Gurtner, G. J., Newberry, R. D., Schloemann, S. R., McDonald, K. G., & Stenson, W. F. (2003). Inhibition of indoleamine 2, 3-dioxygenase augments trinitrobenzene sulfonic acid colitis in mice. *Gastroenterology, 125*(6), 1762-1773.

Hashimoto, T., Perlot, T., Rehman, A., Trichereau, J., Ishiguro, H., Paolino, M., . . . Penninger, J. M. (2012). ACE2 links amino acid malnutrition to microbial ecology and intestinal inflammation. *Nature, 487*(7408), 477-481. doi: 10.1038/nature11228

Huttunen, R., Syrjänen, J., Aittoniemi, J., Oja, S. S., Raitala, A., Laine, J., . . . Hurme, M. (2010). HIGH ACTIVITY OF INDOLEAMINE 2,3 DIOXYGENASE ENZYME PREDICTS DISEASE SEVERITY AND CASE FATALITY IN BACTEREMIC PATIENTS. *Shock, 33*(2), 149-154 110.1097/SHK.1090b1013e3181ad3195.

Itoh, K., Maejima, K., Ueda, K., & Fujiwara, K. (1979). Difference in Susceptibility of Mice Raised under Barrier-Sustained (SPF) or Conventional Conditions to Infectious Megaenteron. *Microbiology and Immunology, 23*(9), 909-913. doi: 10.1111/j.1348-0421.1979.tb02824.x

Johansson, M. E. V., Gustafsson, J. K., Sjoberg, K. E., Petersson, J., Holm, L., Sjovall, H., & Hansson, G. C. (2010). Bacteria Penetrate the Inner Mucus

Layer before Inflammation in the Dextran Sulfate Colitis Model. *PLoS One, 5*(8). doi: 10.1371/journal.pone.0012238

Kang, C. S., Ban, M., Choi, E. J., Moon, H. G., Jeon, J. S., Kim, D. K., . . . Kim, Y. K. (2013). Extracellular Vesicles Derived from Gut Microbiota, Especially Akkermansia muciniphila, Protect the Progression of Dextran Sulfate Sodium-Induced Colitis. *PLoS One, 8*(10), 11. doi: 10.1371/journal.pone.0076520

Kau, A. L., Ahern, P. P., Griffin, N. W., Goodman, A. L., & Gordon, J. I. (2011). Human nutrition, the gut microbiome and the immune system. *Nature, 474*(7351), 327-336.

Kim, C. J., Kovacs-Nolan, J. A., Yang, C. B., Archbold, T., Fan, M. Z., & Mine, Y. (2010). L-Tryptophan exhibits therapeutic function in a porcine model of dextran sodium sulfate (DSS)-induced colitis. *Journal of Nutritional Biochemistry, 21*(6), 468-475. doi: 10.1016/j.jnutbio.2009.01.019

Kitajima, S., Takuma, S., & Morimoto, M. (2000). Histological analysis of murine colitis induced by dextran sulfate sodium of different molecular weights. *Exp Anim, 49*(1), 9-15.

Knights, D., Lassen, K. G., & Xavier, R. J. (2013). Advances in inflammatory bowel disease pathogenesis: linking host genetics and the microbiome. *Gut, 62*(10), 1505-1510.

Lam, Y. Y., Ha, C. W. Y., Campbell, C. R., Mitchell, A. J., Dinudom, A., Oscarsson, J., . . . Storlien, L. H. (2012). Increased Gut Permeability and Microbiota Change Associate with Mesenteric Fat Inflammation and Metabolic Dysfunction in Diet-Induced Obese Mice. *PLoS One, 7*(3), e34233. doi: 10.1371/journal.pone.0034233

Laroui, H., Ingersoll, S. A., Liu, H. C., Baker, M. T., Ayyadurai, S., Charania, M. A., . . . Merlin, D. (2012). Dextran Sodium Sulfate (DSS) Induces Colitis in Mice by Forming Nano-Lipocomplexes with Medium-Chain-Length Fatty Acids in the Colon. *PLoS One, 7*(3), e32084. doi: 10.1371/journal.pone.0032084

Lee, J. H., & Lee, J. (2010). Indole as an intercellular signal in microbial communities. *FEMS Microbiol Rev, 34*(4), 426-444. doi: 10.1111/j.1574-6976.2009.00204.x

Mardis, E. R. (2008). Next-generation DNA sequencing methods *Annual Review of Genomics and Human Genetics* (Vol. 9, pp. 387-402).

Maslowski, K. M., Vieira, A. T., Ng, A., Kranich, J., Sierro, F., Yu, D., . . . Mackay, C. R. (2009). Regulation of inflammatory responses by gut microbiota and chemoattractant receptor GPR43. *Nature, 461*(7268), 1282-U1119. doi: 10.1038/nature08530

Maxwell, J. R., Brown, W. A., Smith, C. L., Byrne, F. R., & Viney, J. L. (2009). Methods of inducing inflammatory bowel disease in mice. *Curr Protoc Pharmacol, Chapter 5*, Unit5.58. doi: 10.1002/0471141755.ph0558s47

Moolenbeek, C., & Ruitenberg, E. J. (1981). The 'Swiss roll': a simple technique for histological studies of the rodent intestine. *Laboratory Animals, 15*(1), 57-59. doi: 10.1258/002367781780958577

Neufeld, K., Kang, N., Bienenstock, J., & Foster, J. (2011). Reduced anxiety-like behavior and central neurochemical change in germ-free mice. *Neurogastroenterology & Motility, 23*(3), 255-e119.

Nguyen, N. T., Kimura, A., Nakahama, T., Chinen, I., Masuda, K., Nohara, K., . . . Kishimoto, T. (2010). Aryl hydrocarbon receptor negatively regulates dendritic cell immunogenicity via a kynurenine-dependent mechanism. *Proceedings of the National Academy of Sciences, 107*(46), 19961-19966.

O'Hara, A. M., & Shanahan, F. (2006). The gut flora as a forgotten organ. *EMBO Rep, 7*(7), 688-693. doi: 10.1038/sj.embor.7400731

Ott, S., Musfeldt, M., Wenderoth, D., Hampe, J., Brant, O., Fölsch, U., . . . Schreiber, S. (2004). Reduction in diversity of the colonic mucosa associated bacterial microflora in patients with active inflammatory bowel disease. *Gut, 53*(5), 685-693.

Pils, M. C., Bleich, A., Prinz, I., Fasnacht, N., Bollati-Fogolin, M., Schippers, A., . . . Müller, W. (2011). Commensal gut flora reduces susceptibility to

experimentally induced colitis via T-cell-derived interleukin-10. *Inflammatory Bowel Diseases, 17*(10), 2038-2046.

Rakoff-Nahoum, S., Paglino, J., Eslami-Varzaneh, F., Edberg, S., & Medzhitov, R. (2004). Recognition of commensal microflora by toll-like receptors is required for intestinal homeostasis. *Cell, 118*(2), 229-241.

Robertson, B. R., O'Rourke, J. L., Neilan, B. A., Vandamme, P., On, S. L., Fox, J. G., & Lee, A. (2005). Mucispirillum schaedleri gen. nov., sp. nov., a spiral-shaped bacterium colonizing the mucus layer of the gastrointestinal tract of laboratory rodents. *International journal of systematic and evolutionary microbiology, 55*(3), 1199-1204.

Russell, W. R., Duncan, S. H., Scobbie, L., Duncan, G., Cantlay, L., Calder, A. G., . . . Flint, H. J. (2013). Major phenylpropanoid-derived metabolites in the human gut can arise from microbial fermentation of protein. *Molecular Nutrition & Food Research, 57*(3), 523-535. doi: 10.1002/mnfr.201200594

Sartor, R. B. (2008). Microbial influences in inflammatory bowel diseases. *Gastroenterology, 134*(2), 577-594.

Shendure, J., & Ji, H. (2008). Next-generation DNA sequencing. *Nat Biotechnol, 26*(10), 1135-1145. doi: 10.1038/nbt1486

Shimada, Y., Kinoshita, M., Harada, K., Mizutani, M., Masahata, K., Kayama, H., & Takeda, K. (2013). Commensal Bacteria-Dependent Indole Production Enhances Epithelial Barrier Function in the Colon. *PLoS One, 8*(11). doi: 10.1371/journal.pone.0080604

Shizuma, T., Mori, H., & Fukuyama, N. (2013). Protective effect of tryptophan against dextran sulfate sodium- induced experimental colitis. *Turk J Gastroenterol, 24*(1), 30-35.

Swidsinski, A., Loening-Baucke, V., Vaneechoutte, M., & Doerffel, Y. (2008). Active Crohn's disease and ulcerative colitis can be specifically diagnosed and monitored based on the biostructure of the fecal flora. *Inflammatory Bowel Diseases, 14*(2), 147-161. doi: 10.1002/ibd.20330

Thorkildsen, L. T., Nwosu, F. C., Avershina, E., Ricanek, P., Perminow, G., Brackmann, S., . . . Rudi, K. (2013). Dominant Fecal Microbiota in Newly

Diagnosed Untreated Inflammatory Bowel Disease Patients. *Gastroenterology research and practice, 2013*.

Troy, E. B., & Kasper, D. L. (2010). Beneficial effects of Bacteroides fragilis polysaccharides on the immune system. *Front Biosci (Landmark Ed), 15*, 25-34.

Wang, Garrity, G. M., Tiedje, J. M., & Cole, J. R. (2007). Naive Bayesian classifier for rapid assignment of rRNA sequences into the new bacterial taxonomy. *Appl Environ Microbiol, 73*(16), 5261-5267. doi: 10.1128/aem.00062-07

Wang, Qiao, S. Y., & Li, D. F. (2009). Amino acids and gut function. *Amino Acids, 37*(1), 105-110. doi: 10.1007/s00726-008-0152-4

Yokoyama, M., & Carlson, J. (1979). Microbial metabolites of tryptophan in the intestinal tract with special reference to skatole. *The American Journal of Clinical Nutrition, 32*(1), 173-178.

Zelante, T., Iannitti, R. G., Cunha, C., De Luca, A., Giovannini, G., Pieraccini, G., . . . Romani, L. (2013). Tryptophan Catabolites from Microbiota Engage Aryl Hydrocarbon Receptor and Balance Mucosal Reactivity via Interleukin-22. *Immunity, 39*(2), 372-385. doi: 10.1016/j.immuni.2013.08.003

국문초록

대장염 모델 *Ido1*$^{-/-}$ 마우스에서의 장내 미생물체 분석

서울대학교 대학원 식품영양학과

신 지 희

차세대 염기서열 분석 기법이 발달함에 따라 인간과 공생하는 미생물에 관한 연구가 활발히 연구되고 있다. 특히 다른 기관에 비해 장내에는 매우 다양한 미생물들이 존재하고 있으며, 숙주의 면역체계와 긴밀한 상호관계를 맺고 있음이 알려져 있다. 선행연구 결과, *Ido1* (indoleamine 2,3-dioxygenase 1; 트립토판 대사의 속도조절 효소)은 미생물 노출 정도의 차이에 따라 발현이 변화한 유전자 중 하나임을 확인하였다. 따라서 본 연구에서는 트립토판 대사를 매개로 한 장내 미생물과 숙주의 염증반응과의 연관성을 밝히고자, *Ido1*$^{-/-}$마우스와 *Ido1*$^{+/+}$마우스를 사용하여 급성 대장염을 유도한 후, 파이로시퀀싱을 이용하여 장내 미생물체 분석을 실시하였다. 마우스는 dextran sodium sulfate (DSS)를 녹인 음용수를 7 일간 마우스에게 공급하여 급성 대장염을 유도하였다. 2% DSS 를 공급한 두 유전자형의 마우스에서 모두 대장염이 유도됐으나 *Ido1*$^{+/+}$

마우스에서 더 심각한 염증이 유도됨을 관찰했다. 특히 DSS 가 직접 영향을 끼치는 대장 조직에서 길이의 감소와 조직학적인 염증이 *Ido1*$^{-/-}$ 마우스에 비해 *Ido1*$^{+/+}$ 마우스에서 유의적으로 더 높게 나타났다. 이어서 파이로시퀀싱 방법을 이용하여 두 유전자형 마우스의 장내 미생물 군집의 차이를 분석하였고, 여덟 가지의 문(phylum)의 상이한 분포를 확인하였다. 흥미롭게도 Bacteroidetes 문(phylum)과 Firmicutes 문(phylum)의 비율이 두 군간에 유의적인 차이를 보였다. 또한 *Ido1*$^{-/-}$ 마우스는 *Bacteroides, Parabacteroides, Barnesiella, Prevotella* 속(genus)이 유의적으로 높은 비율을 차지했다. 이 네 가지 박테리아 중 세 가지는 트립토판을 이용하여 인돌로 대사하는 것으로 알려져 있다. 특히 염증 정도가 높았던 *Ido1*$^{+/+}$ 마우스에서 특이적으로 뮤신을 사용하는 *Mucispirillum* 과 병원성인 *Escherichia/Shigella* 속(genus)이 관찰됐다. 결론적으로 본 연구에서는 트립토판 분해효소 *Ido1* 은 장내 박테리아 조성을 변화시킴으로써 장내 염증 반응 유도에 관여함을 제시하였다. 또한 숙주와 장 속에 공존하는 미생물체는 서로 영양소 대사 네트워크를 공유함으로써 서로 커뮤니케이션을 할 수 있다는 하나의 예를 제시하는 것으로 사료된다.

주요어: 마이크로바이옴, Indoleamine 2,3-dioxygenase 1 (*Ido1*), 트립토판, 파이로시퀀싱, Dextran sodium sulfate (DSS), 대장염

학번: 2012-21496